Roughness variability estimation of microscopic surfaces during engineering wear process-Application to total hip implant

Ola Suleiman Ahmad, Yann Gavet, Jean Geringer, Jean-Charles Pinoli

Roughness variability estimation of microscopic surfaces during engineering wear process- Application to total hip implant

Ola Suleiman Ahmad, Yann Gavet, Jean Geringer, and Jean-Charles Pinoli
LGF, UMR CNRS 5037
Ecole Nationale Supérieure des Mines de Saint-Etienne
158 cours Fauriel, 42023, Saint-Etienne, France
Email: gavet@emse.fr

This paper proposes a new method to estimate the roughness changes from topographic features of microscopic surfaces during an engineering wear process. We demonstrate that the evolution of the significant upcrossings of surface topography is the most efficient way to estimate the roughness changes associated with the small-scale changes during the time of wear process. The motivation of this work comes from the fact that the surface roughness is, largely, interpolated with many important mechanical and physical phenomena, such as friction, and wear behaviour during the mechanical contact between joined and sliding surfaces. A special application is investigated on UHMWPE (Ultra High Molecular Weight Polythene) components involved in total hip implants. The aim is to understand the *in-vitro* wear mechanism of the UHMWPE surface by estimating its roughness evolution.

1 introduction

In the total hip replacement, a dual mobility concept is used to replace the hip joint (see Fig. 1). The prosthetic implant consists of a femoral stem with a femoral head placed on the upper part of the stem, made of stainless steel, a socket (acetabular) in place of the acetabulum (the cartilage surface of the socket), and a dual mobility cup inserted between the ball and the socket to provide the convenient motion that allows for a very stable articulation [1]. The dual mobility cup that is commonly used in the hip replacement is the UHMWPE (Ultra High Molecular Weight PolyEthylene) component, due to its low friction coefficient, and its hardness that makes it an ideal bearing surface for the articulation between the ball and the socket. However, it has an inconvenient associated with its low resistance to the wear. The wear particles (debris) produced by sliding the UHMWPE liner against other articulated surfaces will accelerate the material's loosening, which is one of the main limiting factors

of the life of the arthroplasty. On the other hand, the produced debris affects strongly the bone structure, [2], such as changing the osteoclast, and osteoblast activity which might lead to the bone resorption and other non expected effects. Thus, a geometric and morphological characterizations of the UHMWPE component during engineered wear process would help understanding the *in-vitro* wear mechanism, and the tribological behaviour (lubrication, wear volume,....) of such materials. This is one of the critical issues related with improving the performance and the life duration of the implant.

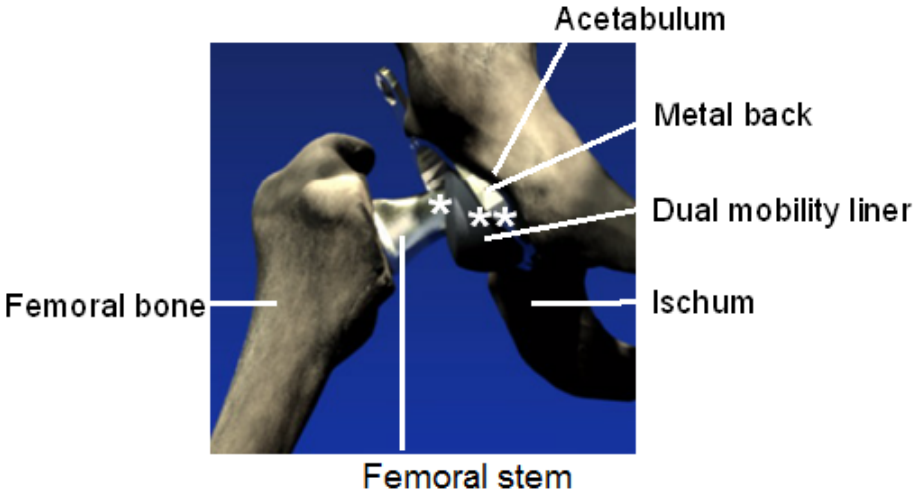

Figure 1: An illustration of the the dual mobility concept involved in the total hip implant [3]. The white stars in the plot refer to the prosthetic components : Metal back, dual mobility liner, and the femoral stem.

The topographic map of microstructure surfaces extends across large and small scales to be composed of, roughly speaking, form, waviness, and roughness components [4]. During wear (generally engineering) process, the geometry of the topographical features will deform dependently over multiple spatial scales. Nevertheless, the small-scale features (the roughness component) referred to the local maxima and minima of the surface will change instantaneously. Thus, the roughness evolution of the surface will govern many important physical phenomena, specifically in this paper, the wear mechanisms during the mechanical contact between sliding surfaces. Towards estimating the roughness evolution, the mathematical representation of the surface roughness topography becomes the essential step, that can be investigated by different approaches according to the measurement technique methods, [4–7]. The focus of the present paper concerns on the topographic map of microstructure surfaces measured by a 3D non-contact optical instrumentation techniques, known by optical interferometry. The surface is, then, considered as a 3D height map, also it can be represented as a 2D image, digitized on a rectilinear lattice in the measurement space.

Thereby, image processing and mathematical imaging based-methods can be applied to analyse and model the surface topography, for estimating the surface roughness, such as multi-scale methods [6, 8–11], geometric methods [12–17], and the statistical methods [18–24]. Due to the random nature of microscopic surfaces, a statistical analysis based on a well established stochastic geometrical model will be the best solution to estimate the surface roughness, and the geometry of the hills when the UHMWPE surface slides against a smooth metal one. Such models are dedicated by the random fields framework and their geometry [25, 26].
This paper represents the surface roughness topography as a skew$-t$ random field. We are interested in studying the geometric structure of the excursion sets of the skew$-t$ random field at high thresholds in order to estimate its local maxima and minima (hills and valleys), and the roughness variability during the *in-vitro* wear engineering process conducted by a hip simulator device.

2 Experimental setup

2.1 Wear test

The wear tests are conducted by a one-station hip wear simulator, 858 Mini Bionix® II test system (MTS), in experimental environment corresponding to the dynamic conditions of the human joint movement. The hip wear simulator, illustrated in Fig. 2, is provided by three electric motors on the X,Y, Z axes which generate three time-varying angular displacements with the walking cycles and simulate the hip-joint movement. The force load is held on the Z axis and it varies between 300N to 3KN according to the normative reference ISO 14242-1. The hip implant solution is based on the dual mobility concept, [1], and it consists of a UHMWPE (Ultra High Molecular Weight Polyethylene) cup, femoral head, femoral stem and acetabular cup which are made of stainless steel (316L SS). The UHMWPE component is articulated with the femoral head and the acetabular cup which offers the dual mobility of the UHMWPE cup. All the hip implant components are completely immersed in a fluid test medium that contains a physiological liquid of calf serum at a controlled temperature of $37^\circ \pm 2^\circ C$. The serum liquid has to be replaced every 5×10^5 cycles, and the measurements are taken at every 1×10^6 cycles ($\simeq 300$ hours).

2.2 Surface roughness measurements

The UHMWPE surface has been measured, locally, by a 3D non-contact white light interferometer, (Bruker nanoscope (r), Wyko® NT 9100, ex. Veeco). The surface samples are digitized and transformed to 3D height maps which are represented on a lattice of 480×640 pixels with spatial resolution equal to $\tau_x = 1.8\mu m$, and $\tau_y = 1.8\mu m$ in both X and Y directions, respectively, for each

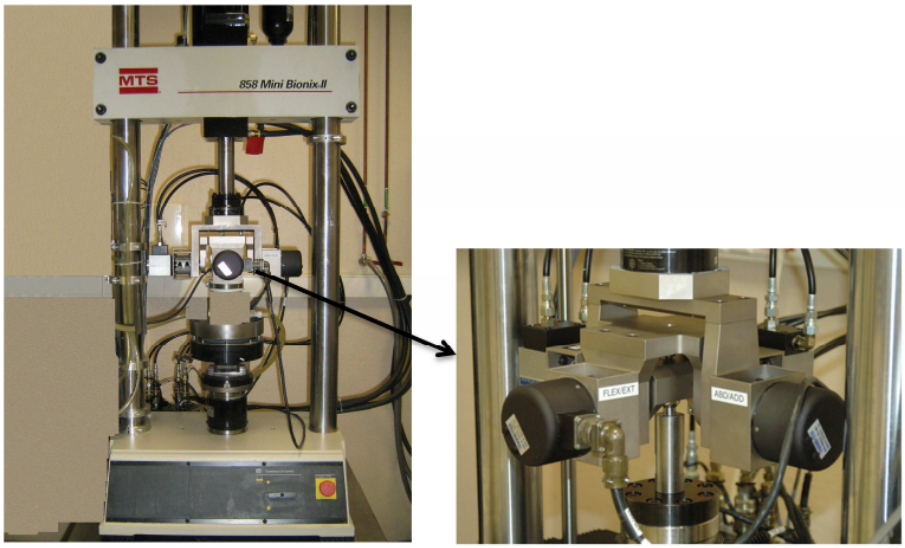

Figure 2: (a) General view of the one-station hip wear simulator. (b) Detail view of the test axes and the hip implant position.

pixel, (see Fig. 3).
Since, the optical instrument provides local measurements of the UHMWPE surface, different regions should be measured during wear process. The certainty of the statistical analyzes lies on the number of treated samples and the size of the measurement space. The maximum measurement space provided by the instrument is $1.1 \times 0.9mm^2$, where the outside diameter of the UHMWPE is $37mm$ [3].
The surface roughness map showed in Fig. 3(b) refers to a local region of the UHMWPE component observed before the start of the wear tests.

3 Methods and developments

A statistical analysis method based on the model of the microscopic surface topography is proposed. The model is defined from a class of elliptical skew random fields with extrema of conical shapes, namely skew student's t random field. This model is considered more flexible than the usual Gaussian random fields that are widely used in the literature to represent the topography of rough surfaces [18–20].

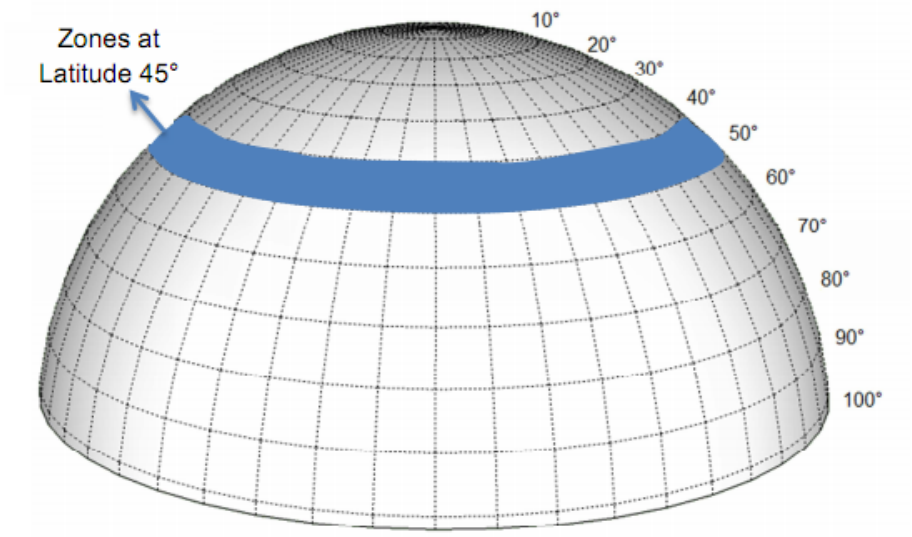

(a)

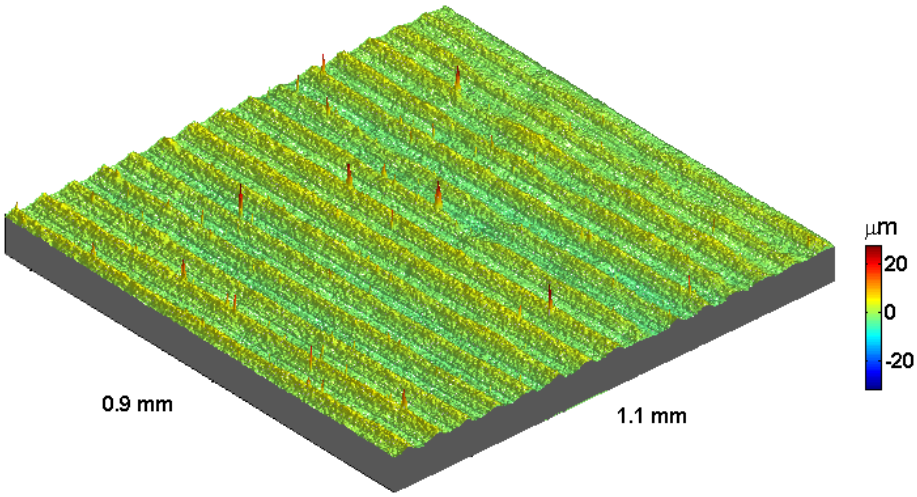

(b)

Figure 3: (a). A synthetic 3D-dimensional model of the UHMWPE dual mobility cup. The blue colored zone refers to the latitude 45°. (b) A 3D height map measured from a local region, at the 45° latitude on a maximum area of $1.1 \times 0.9mm^2$

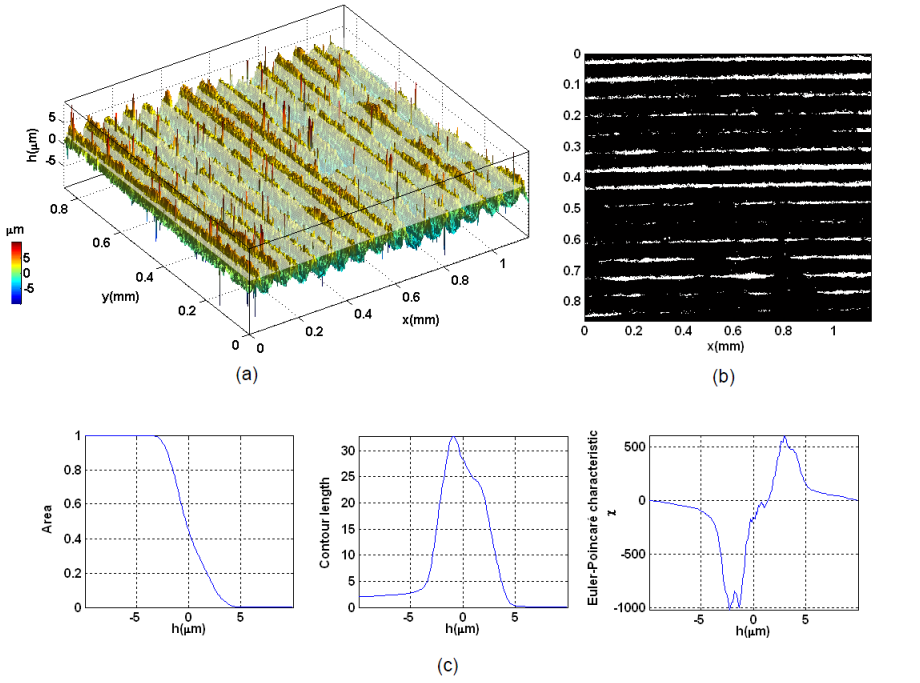

Figure 4: (a) An example of a real 3D surface topography measured from the UHMWPE component. (b) The excursion set obtained at a level threshold $h = 2.5\mu m$ and represented as a 2D binary image. (c) Minkowski functionals (area , contour length, and Euler-Poincaré characteristic χ functions), computed on the binary excursion sets, versus the height levels.

3.1 Surface characterization using integral geometry

The geometric characteristics of the surface topography can be derived from the integral geometry framework, precisely, they are defined by the three characterizing functions namely Minkowski functionals, or Lipschitz-Killing curvatures, referring to the area function, contour length function (edges), and Euler-Poincaré characteristic, that counts the number of connected components minus the number of holes, [27]. These characterizing functions are computed on binary level sets, namely excursion set [26]. Each excursion set is obtained from thresholding the surface heights at a level threshold h, and take all the points at which the surface height exceeds h, (see Fig 4).

The advantage of these functions comes from their physical interpretations. The normalized area function is the material bearing area ratio, notably by Abbott-Firestone curve [28]. The contour length function is related to the distribution of the surface heights, and it describes the shape of the distribution function (the peakedness, and the asymmetry). Euler-Poincaré characteristic

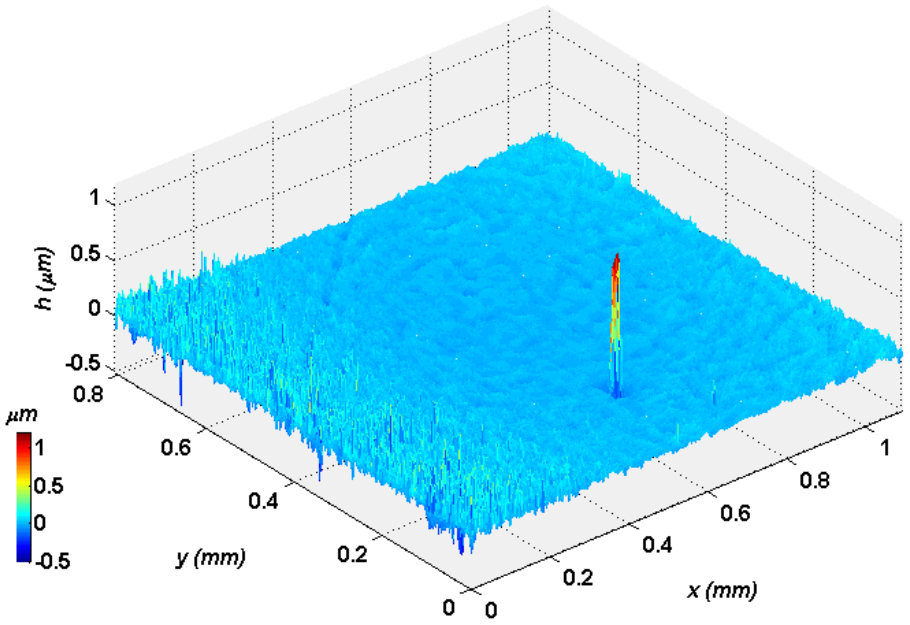

Figure 5: A 3D topography map observed from a worn UHMWPE component during wear process time, defined on a lattice of 480×640 pixels with spatial resolution $\Delta x = 1.8\mu m$, and $\Delta y = 1.8\mu m$.

function has a special interest since it describes the roughness rate of the surface, and the behaviour of its extrema. At the high thresholds it estimates the number of the connected components, associated with the surface hills and valleys [26], as will be seen further in the paper.

3.2 Surface roughness representation

Let Y be the 3D topography map of a worn surface, (see Fig 5). The Q-Q plot of the surface heights versus the normal distribution (see Fig 6) assures that the height's distribution is not a normal one. It follows a normal curve fairly closely within a small interval around its mean value, conversely to its extremes which are quite far from normality. Furthermore, the surface heights exhibit asymmetry behaviour, around their mean value, which incorporates the concept of the skewness in the distribution function. Accordingly, the height's of the real surface are suggested to follow a skew student's t distribution. Due to the spatial dependence between the surface heights, they are modelled as a two-dimensional stationary skew student's t random field.
A two-dimensional stationary skew student's t random field, denoted $\{Y(s)$:

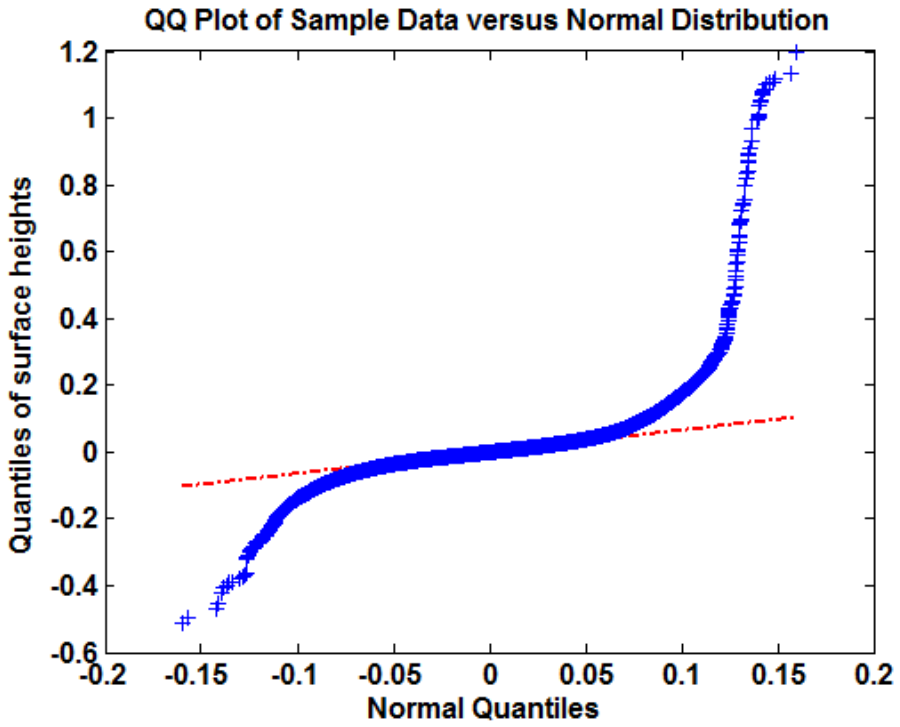

Figure 6: Normal Q-Q plot of the surface heights (blue curve) versus the normal distribution (red line). The heights are negatively skewed with centered and heavy-tailed distribution of mean value $\mu = 5.37nm$, standard deviation $\sigma = 34nm$, skewness $S_{sk} = 4.41$, and kurtosis $S_{ku} = 111.81$

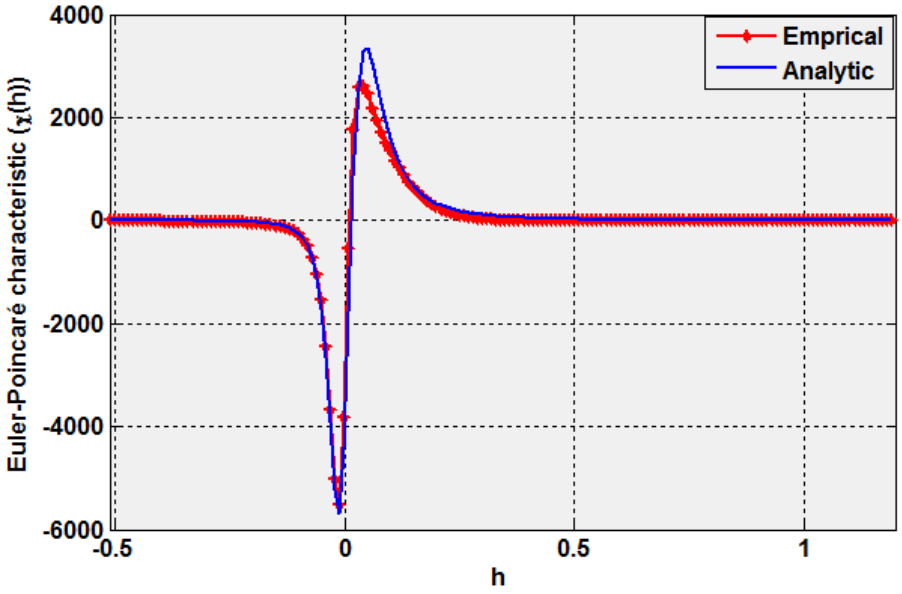

Figure 7: Fitting the estimated and the expected Euler characteristics of the real measurements and the skew student's t random field with $k = 10$ degrees of freedoms and $\delta = 0.7$, $\sqrt{\det(\Lambda)} = 179\mu m^{-2}$.

$s \in S\}$, is defined, at any fixed point s in the measurement space S, as follows:

$$Y(s) = \frac{\delta|z| + \sqrt{1-\delta^2}Z_0(s)}{\left(\frac{1}{k}\sum_{i=1}^{k} Z_i^2(s)\right)^{1/2}} \tag{1}$$

where $(\delta^2 < 1)$ denotes the skewness index, $Z_0, ..., Z_k$ are independent and identically distributed Gaussian random fields with the diagonal spectral moments matrix, denoted by (Λ). $z \sim N(0,1)$ is a standard normal variable independent of Z_i, $i = 0, ..., k$, and k is the degree of freedoms of Y.
The geometry of the skew$-t$ random field is identified by the integral geometry of its excursion sets. An excursion set, denoted $E_h(Y,S)$, of a random field Y on a subset S, is defined by the set of the points s in S at which Y exceeds a selected threshold h, such that:

$$E_h(Y,S) = \{s \in S : Y(s) \geq h\} \tag{2}$$

The expected Euler-Poincaré characteristic of $E_h(Y,S)$ for the skew student's t random field near its extrema (at high thresholds) is derived in [29], and it is

expressed, at h, as follows:

$$\mathbb{E}\{\chi(E_h(Y,S))\} \cong \frac{2Area(S)\sqrt{\det(\Lambda)}\Gamma\left(\frac{k+1}{2}\right)}{(2\pi)^{3/2}(\sqrt{k/2})\Gamma\left(\frac{k}{2}\right)} h\left(1+\frac{h^2}{k(1-\delta^2)}\right) \times \left(1+\frac{h^2}{k}\right)^{-\frac{k+1}{2}} T_1\left(\alpha h\sqrt{\frac{k+1}{h^2+k}}; k+1\right) \tag{3}$$

where $\Gamma(.)$ is the gamma function, $Area(S)$ is the area of the measurement space $(1.1\times 0.9mm^2)$, and T_1 is the cumulative student's t distribution of $k+1$ degrees of freedoms.

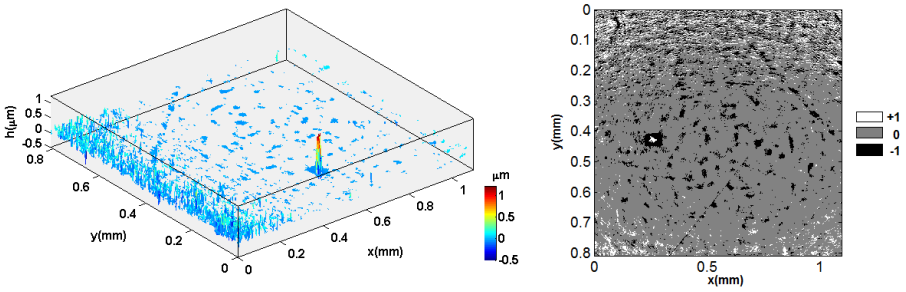

Figure 8: Combination of the significant excursion sets of the sample roughness topography at wear process time 13×10^6. (a) The surface hills and valleys elevations above and below h_1, h_2, respectively. (b) The discrete mapping function I of the excursion set E_{h_1,h_2}. The clusters above the positive threshold h_1 are given the value $(+1)$ and the clusters indicated below the negative threshold h_2 are given the value (-1).

3.3 Parameters estimation

The model's parameters are estimated from fitting the analytical Euler-Poincaré characteristic of the skew student's t excursion sets with the empirical one, computed from the real surface upcrossings, using the non-linear least square minimization, see Fig 7, such that $\delta = 0.7$, $\det(\Lambda)^{1/2} = 179\mu m^{-2}$, and $k = 10$, for the example in Fig 5.

3.4 Estimation of roughness variability during wear process

The surface extrema at high thresholds follow a skew student's t random field, thus, the expected Euler-Poincaré characteristic, expressed in Eq. 3, is used to control the threshold, h, at which the surface upcrossing can be considered as collection of the significant disjoint regions (connected components) that refer

to the hills and valleys.
The main reason come from the fact that the probability of detection a maxima of Y above a threshold h is approximated by the mean Euler-Poincaré characteristic, [26], such as:

$$\mathbb{P}[Y_{max} > h] \approx \mathbb{E}\{\chi(E_h(Y,S)),\ \ (h \to \infty) \tag{4}$$

Notice that the same contribution can be considered for the minima of Y too. Consequently, the threshold h is chosen such that the probability of detecting significant regions (hills or valleys) above very high threshold h (near the global maxima/minima) do not exceed 5%. So, all the surface upcrossings above h can be ignored or rejected.

Let consider $h_1 > 0$ and $h_2 < 0$ be the significant detected upcrossings, inferred to the excursion sets, E_{h_1} and E_{h_2}, including the hills and valleys, respectively. A discrete mapping function $I\left(E_{(h1,h2)}\right)$ is then defined on the joint excursion set $E_{(h1,h2)}$, to enable visualizing the surface hills/valleys, (see Fig. 8(a)), such that:

$$I\left(E_{(h1,h2)}\right) = \begin{cases} +1, & if\ x \in E_{h_1} \\ -1, & if\ x \in E_{h_2} \end{cases} \tag{5}$$

as seen in Fig. 8(b).
Fig 9 illustrates the significant surface upcrossings estimated for a sample of the UHMWPE component during wear process time. The surface upcrossings at h_1 and h_2 are associated with the evolution of the peak materials and valleys material portions during wear time. They show an obvious degradation of the surface heights during the wear process, except at the wear time 6×10^6 cycles, in both h_1 and h_2 plots, there is an unexpected spikes due to the measurement errors.
Furthermore, computing the difference between the spatial extents of the detected hills/valleys at the significant upcrossings h_1 and $|h_2|$ during the time can express the roughness variability of the surface topography as a function with time, such that:

$$f(t) = h_1(t) \times Area[E_{h_1(t)}(s)] - |h_2(t)| \times Area[E_{h_2(t)}(s)] \tag{6}$$

where $f(t)$ is the function of the roughness variations during time.

4 Results and discussion

The roughness evolution function are estimated, during wear process time across 19×10^6 cycles, for 5 selected samples measured from the UHMWPE component at latitude 45°, (see Fig 10). The results in Fig 10 demonstrate that the functional behaviour during wear process can be considered homogeneous around the same latitude of the worn UHMWPE component. Nevertheless, more statistical results should be performed on the UHMWPE component at different

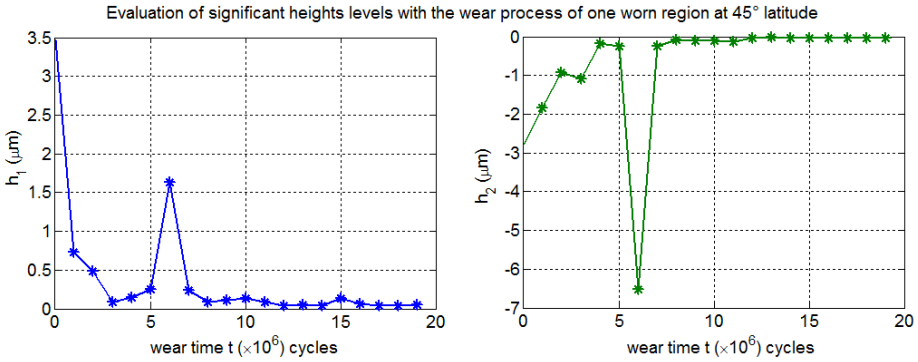

Figure 9: Detection of significant peaks and valleys levels, h_1 and h_2, respectively, of a sample measured from the UHMPWE at 45° latitude along 19×10^6 cycles of wear time

latitudes over more regions, to insure this assumption. Furthermore, the roughness permutations, in the period between 4×10^6 to 12×10^6 cycles, describe the existence of a complex wear mechanisms derived from combined abrasive (or erosion) and adhesive wears, as expected experimentally.

On the other hand, the evolution of the significant upcrossings during time 8 samples measured at different longitudes, 4 samples around the latitude 45°, and 4 samples around the latitudes 100°, (see Fig 11), illustrates the significant difference between the behaviour of the UHMWPE regions along its longitudes, and demonstrates that the significant material loosening during wear time, and the wear effect, governs the upper part of the UHMWPE. The last conclusion might be promising to generate a dual mobility cup of non homogeneous materials, for improving the quality of the implant.

5 Conclusion

This paper highlights the importance of the mathematical modelling for analysing and describing the roughness changes during the engineering wear of a surface. The Q-Q plot demonstrates that the heights distribution is skewed and heavily tailed, so it can not be considered as a Gaussian one, and might follow a skew student's t random field.

A particular research, representative by the UHMWPE component involved in the total hip replacement, is investigated in this paper. The roughness evolution during wear time is estimated using the expected Euler-Poincaré characteristic as a function of the difference between the spatial extents of the surface upcrossings multiplied by their height's levels.

The paper is focused on the estimation of the surface roughness evolution at each fixed time along the wear process. Thus, our aim at the future work is to combine both the spatial and the temporal roughness descriptors using the

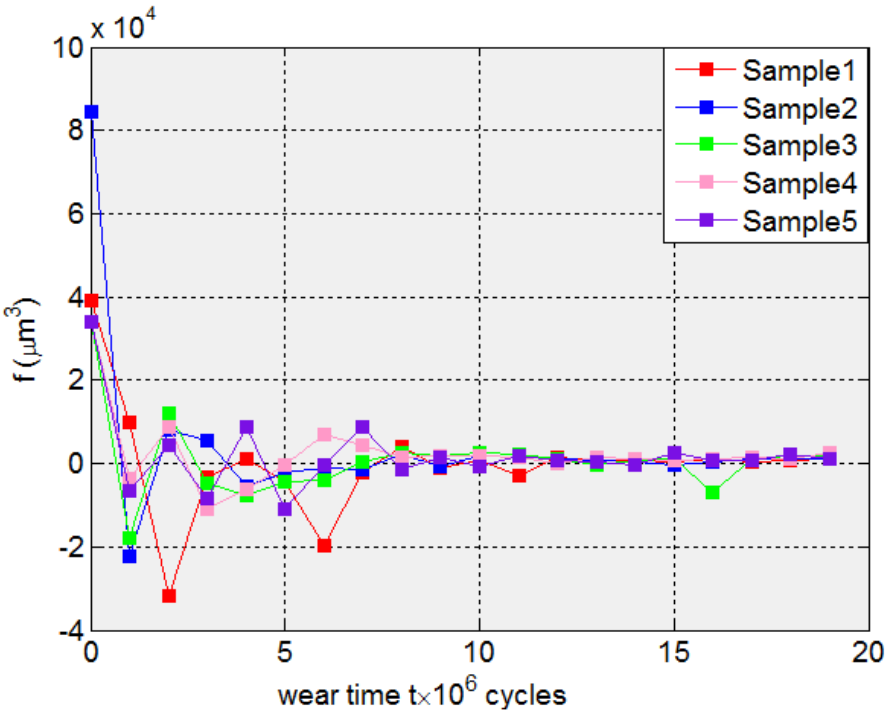

Figure 10: The global area of the disjoint clusters multiplied by the significant levels, f, versus wear time for the selected 5 UHMWPE samples.

space-time random fields.

Acknowledgment

The authors would like to thank Serf Dedienne Santé company, for providing the prosthetic femoral implants and the UHMWPE component. Also the authors would acknowledge Mr. Nicolas Curt in the École Nationale Supérieure des Mines de Saint-Etienne for his technical assistance in preparing the required materials for the experimentations.

References

[1] G. Bousquet, D. Gazielly, P. Girardin, J. Debiesse, M. Relave, and A. Israeli, "The ceramic coated cementless total hip arthroplasty. basic concepts and surgical technique," *Journal of Orthopaedic surgery*, vol. 1, pp. 15–28, 1985.

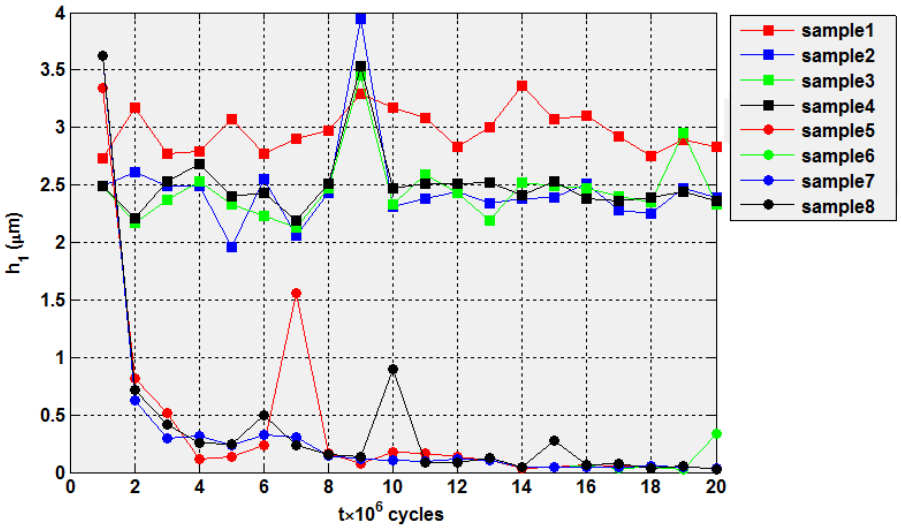

(a)

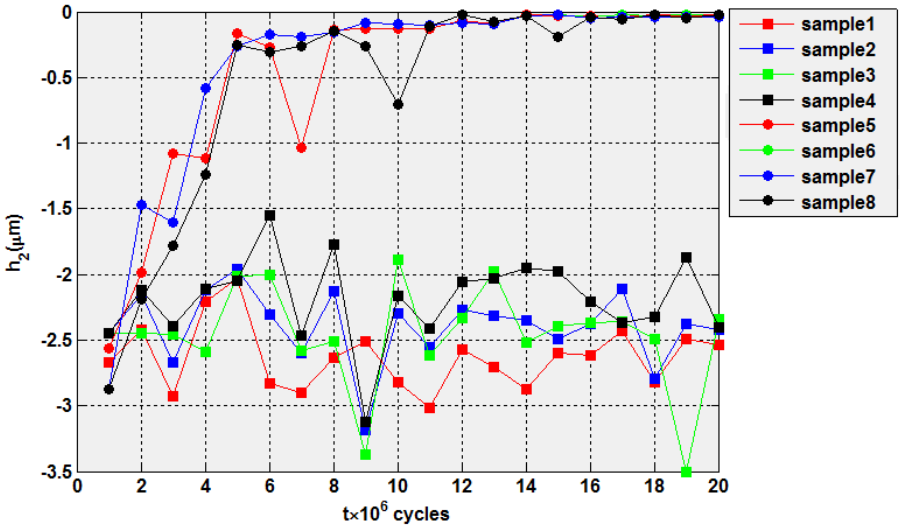

(b)

Figure 11: A quantitative comparison between the regions of the UHMWPE component measured from longitudes 45° and 100° showing different degree of wear. (a) The hills levels at h_1. (b) The valleys levels at h_2. The samples from *sample*1 to *sample*4 are measured along the latitude 100°. The samples from *sample*5 to *sample*8 are measured along the latitude 45°.

[2] C. Figueiredo-Pina, P. Dearnley, and J. Fisher, "UHMWPE wear response to apposing nitrogen s-phase coated and uncoated orthopaedic implant grade stainless steel," *Wear*, vol. 267, no. 5-8, pp. 743 – 752, 2009.

[3] J. Geringer, B. Boyer, and F. Farizon, "Understanding the dual mobility concept for total hip arthroplasty. investigations on a multiscale analysis-highlighting the role of arthrofibrosis," *Wear*, vol. 271, no. 9 - 10, pp. 2379 – 2385, 2011.

[4] X. Jiang, P. Scott, D. Whitehouse, and L. Blunt, "Paradigm shifts in surface metrology. part II. the current shift," *Proceedings of the Royal Society A: Mathematical, Physical and Engineering Science*, vol. 463, no. 2085, pp. 2071 – 2099, 2007. [Online]. Available: http://rspa.royalsocietypublishing.org/content/463/2085/2071.abstract

[5] H. Kesari and A. J. Lew, "Effective macroscopic adhesive contact behavior induced by small surface roughness," *Journal of the Mechanics and Physics of Solids*, vol. 59, no. 12, pp. 2488 – 2510, 2011. [Online]. Available: http://www.sciencedirect.com/science/article/pii/S0022509611001487

[6] J. Schmähling, "Statistical characterization of technical surface microstructure," Ph.D. dissertation, Ruprecht-Karls University, Heidelberg, 2006.

[7] W. P. Dong and K. J. Stout, "An integrated approach to the characterization of surface wear i: Qualitative characterization," *Wear*, vol. 181-183, no. Part 2, pp. 700 – 716, 1995, 10th International Conference on Wear of Materials. [Online]. Available: http://www.sciencedirect.com/science/article/B6V5B-49XYXJY-16/2/f010716543dced4b9b3e134ccf70c5a7

[8] Y. Wang and K. S. Moon, "A methodology for the multi-resolution simulation of grinding wheel surface," *Wear*, vol. 211, no. 2, pp. 218 – 225, 1997.

[9] Y. Lin, X. R. Xiao, X. P. Li, and X. W. Zhou, "Wavelet analysis of the surface morphologic of nanocrystalline tio2 thin films," *Surface Science*, vol. 579, no. 1, pp. 37 – 46, 2005.

[10] B. Josso, D. R. Burton, and M. J. Lalor, "Frequency normalised wavelet transform for surface roughness analysis and characterisation," *Wear*, vol. 252, no. 5-6, pp. 491–500, Mar. 2002.

[11] M. Dietzsch, M. Gerlach, and S. Grger, "Back to the envelope system with morphological operations for the evaluation of surfaces," *Wear*, vol. 264, no. 56, pp. 411 – 415, 2008.

[12] H. Zahouani, R. Vargiolu, and J. L. Loubet, "Fractal models of surface topography and contact mechanics," *Mathematical and Computer Modelling*, vol. 28, no. 4-8, pp. 517 – 534, 1998.

[13] R. S. Sayles and T. R. Thomas, "Surface topography as a non-stationary random process," *, Published online: 02 February 1978; doi:10.1038/271431a0*, vol. 271, no. 5644, pp. 431–434, Feb. 1978.

[14] J. C. Russ, *Fractal Surfaces*. Springer, Feb. 1994.

[15] P. Podsiadlo and G. W. Stachowiak, "Scale-invariant analysis of wear particle surface morphology i: Theoretical background, computer implementation and technique testing," *Wear*, vol. 242, no. 1-2, pp. 160–179, Jul. 2000.

[16] P. Podsiadlo and G. Stachowiak, "Applications of hurst orientation transform to the characterization of surface anisotropy," *Tribology International*, vol. 32, no. 7, pp. 387 – 392, 1999.

[17] Y. F. Peng and Y. B. Guo, "An adhesion model for elastic-plastic fractal surfaces," *Journal of Applied Physics*, vol. 102, no. 5, pp. 053 510 –053 510–7, Sep. 2007.

[18] R. Reizer, "Simulation of 3d gaussian surface topography," *Wear*, vol. 271, no. 3-4, pp. 539 – 543, 2011.

[19] P. Nayak, "Random process model of rough surfaces in plastic contact," *Wear*, vol. 26, no. 3, pp. 305 – 333, 1973. [Online]. Available: http://www.sciencedirect.com/science/article/pii/0043164873901853

[20] J. A. Greenwood and J. B. P. Williamson, "Contact of nominally flat surfaces," *Proceedings of the Royal Society of London. Series A, Mathematical and Physical Sciences*, vol. 295, no. 1442, pp. 300–319, Dec. 1966.

[21] Y. Hu and K. Tonder, "Simulation of 3d random rough surface by 2d digital filter and fourier analysis," *International Journal of Machine Tools and Manufacture*, vol. 32, no. 1-2, pp. 83 – 90, 1992.

[22] J.-J. Wu, "Simulation of rough surfaces with fft," *Tribology International*, vol. 33, no. 1, pp. 47 – 58, 2000.

[23] Y. Ao, Q. Wang, and P. Chen, "Simulating the worn surface in a wear process," *Wear*, vol. 252, no. 1-2, pp. 37 – 47, 2002.

[24] K. Manesh, B. Ramamoorthy, and M. Singaperumal, "Numerical generation of anisotropic 3d non-gaussian engineering surfaces with specified 3d surface roughness parameters," *Wear*, vol. 268, no. 11-12, pp. 1371 – 1379, 2010.

[25] A. M. Yaglom, *Correlation Theory of Stationary and Related Random Functions: Volume I: Basic Results*, 1st ed. Springer, Jun. 1987.

[26] R. J. Adler, *The Geometry of Random Fields (Wiley Series in Probability and Statistics)*. John Wiley & Sons Inc, June 1981.

[27] K. R. Mecke, *Integral Geometry in Statistical Physics.* International Journal of Modern Physics, 1998, vol. 12, no. 9.

[28] E. J. Abbott and F. A. Firestone, "Specifying surface quality: a method based on accurate measurment and comparision," *Mechanical Engineering*, vol. 55, pp. 569–572, 1933.

[29] O. S. Ahmad and J.-C. Pinoli, "Lipschitz-killing curvatures of the excursion sets of skew student' s t random fields," *Stochastic Models*, vol. "", pp. "–", 2013, to appear.